PHYSICAL REVIEW A VOLUME 27, NUMBER 6 JUNE 1983

Quantum theory of optical bistability. III. Atomic fluorescence in a low-Q cavity

H. J. Carmichael and D. F. Walls
Department of Physics, University of Waikato, Hamilton, New Zealand

P. D. Drummond
Department of Physics and Astronomy, University of Rochester, Rochester, New York 14627

S. S. Hassan
Department of Applied Mathematics, Ain Shams University, Abassca, Cairo, Egypt
(Received 18 May 1982)

We specialize the quantum-statistical theory of optical bistability developed in "Optical Bistability. II" to a low-Q cavity. From a linearized Fokker-Planck equation derived in the positive P representation, the steady-state correlation matrix and spectrum of fluctuations are calculated. Expressions which normally assume a positive-definite diffusion matrix are shown to be valid for nonpositive-definite diffusion. For absorptive bistability we find agreement with results derived previously by quite different methods. More generally we extend previously published results by including atomic and cavity detunings. We compare the transmitted spectrum for dispersive bistability with that for absorptive bistability, and photon antibunching in dispersive bistability is discussed.

I. INTRODUCTION

In the preceding paper of this series[1] (hereafter referred to as OBII), a quantum-statistical model for optical bistability was developed. A system of homogeneously broadened two-level atoms interacting with a single driven cavity mode (mean-field limit[2,3]) was considered. Cavity and atomic detunings were included to provide a treatment for both absorptive and dispersive bistability. Radiative and collisional damping of the atoms, and losses at the cavity mirrors, were modeled by coupling the atoms and cavity mode to thermal reservoirs, and a Fokker-Planck equation was derived following Haken's treatment of the laser.[4] With the use of the standard representation of laser theory the resulting equation did not have positive-definite diffusion, but it could be interpreted within the context of the generalized representations introduced by Drummond and Gardiner[5] where positive-semidefinite diffusion can be assured.

In OBII atomic variables were adiabatically eliminated via an Îto stochastic differential equation equivalent to the Fokker-Planck equation, and a theory for optical bistability in a high-Q cavity was developed. In the present paper we treat the low-Q limit where cavity field variables are eliminated. From a linearized theory of fluctuations we calculate the incoherent intensity, spectrum, and second-order correlation function for the transmitted light.

Quantum-statistical treatments of absorptive bistability in a low-Q cavity have been published by Agarwal *et al.*[6] and Lugiato.[7] Agarwal *et al.* begin with a master equation with the cavity field eliminated and derive quantum Langevin equations for atomic operators. They perform a system-size expansion to calculate steady-state correlations and the transmitted spectrum. Their results are shown to correspond to those obtained using the quantum-regression theorem and a Gaussian decoupling approximation.[8] Lugiato[7] arrives at the same results from a linearized Fokker-Planck equation derived in the Wigner (or Weyl) representation. His formalism has also been used to calculate the second-order correlation function[9] and to show that photon antibunching[10] occurs in absorptive bistability.

A quantum-statistical treatment for a low-Q cavity including dispersion has been presented by Agarwal and Tewari.[11] They follow the method of Agarwal *et al.*[6] after adding a term describing atomic detuning to the master equation. They do not, however, include a cavity detuning, and therefore do not give a full description for dispersive bistability. The first objective of our paper is to complement the existing literature by presenting a general quantum-statistical theory for both absorptive and dispersive bistability in a low-Q cavity including both atomic and cavity detunings.

In addition, this calculation provides an illustration of the use of the positive P representation[5] in a circumstance where more familiar techniques—following Haken's laser theory[4]—lead to a Fokker-Planck equation with nonpositive-definite diffusion. Haken uses a representation based on normally ordered operators to transform an operator master equation into a c-number equation. Gronchi and Lugiato[12] and Agarwal *et al.*[13] note that this method leads to a Fokker-Planck equation with nonpositive-definite diffusion and, moreover, that the scaling argument used by Haken to drop the offending terms does not work for optical bistability. They circumvent this problem with a Fokker-Planck equation based on symetric (or Weyl) ordering—an equation for the Wigner (or Weyl) distribution function. This equation has positive-definite diffusion.

Drummond and Gardiner have described a new class of representations, closely associated to that used by Haken, with the usual integration measure extended from the real line into the complex plane.[5] In particular, the positive P representation ensures a positive distribution function and positive-semidefinite diffusion. For this it does impose a cost: The distribution function is now defined in twice as many dimensions. However, in a linearized theory, steady-state moments and the spectrum of fluctuations can be calculated in the original space by a naive application of familiar formal expressions to a Fokker-Planck equation with nonpositive-definite diffusion. The positive P representation merely justifies this procedure. For the special case of absorptive bistability we show that our results, obtained in this way, reduce to those of Agarwal *et al.*[6] and Lugiato.[7]

In Sec. II, we briefly review the model from OBII and derive the linearized Fokker-Planck equation for a low-Q cavity. Steady-state correlations and the spectrum of the transmitted light are derived and discussed in Secs. III and IV, respectively. For absorptive bistability recent calculations by Carmichael[14] and Lugiato[15] have shown that fluorescence perpendicular to the cavity axis has the familiar spectrum of single-atom resonance fluorescence.[16,17] In Sec. V, we briefly review the results of Ref. 14 and their generalization to dispersive bistability. The second-order correlation function is derived in Sec. VI and photon antibunching is found for a wide range of atomic and cavity detunings. Our results and conclusions are summarized in Sec. VII.

II. MODEL AND LINEARIZED THEORY OF FLUCTUATIONS

We consider a two-level homogeneously broadened medium coupled to a single quantized ring-cavity mode excited by a classical driving field. The ring cavity has input and output mirrors aligned in the z direction, each with a reflective coefficient R, where phase changes ϕ_T and ϕ_R accompany transmission and reflection, respectively. The remaining mirrors are perfect reflectors and define a cavity round-trip distance denoted $L+\hat{L}$, where L is the distance of propagation in the medium. The driving (input) field

$$\vec{\mathrm{E}}_i(z,t)=\vec{\mathrm{e}}\mathscr{E}_i e^{i(\omega_0 t-k_0 z)}+\mathrm{c.c.} \tag{2.1}$$

with frequency ω_0, polarization $\vec{\mathrm{e}}$, and amplitude $\mathscr{E}_i$, excites a cavity mode with resonant frequency ω_c. The quantized cavity field is written

$$\vec{\mathrm{E}}(z,t)=i\vec{\mathrm{e}}(\hbar\omega_c/2\epsilon_0 V_Q)^{1/2}\times[a(t)e^{ik_c z}-a^\dagger(t)e^{-ik_c z}]\ , \tag{2.2}$$

where $a^\dagger$ and a are photon creation and annihilation operators, V_Q is the quantization volume, and ϵ_0 is the vacuum permittivity (mks units are used throughout). The medium comprises N two-level atoms, with resonant frequency ω_a and dipole moment $\vec{\mu}(\mu=\vec{\mathrm{e}}\cdot\vec{\mu})$, distributed with uniform density at fixed positions z_j, $j=1,\ldots,N$, throughout an interaction volume $V_I=V_Q L/(L+\hat{L})$. Collective atomic operators are defined by

$$\begin{aligned} J_\pm&=\sum_{j=1}^{N} e^{\pm ik_c z_j}\sigma_\pm^j\ ,\\ J_z&=\sum_{j=1}^{N}\sigma_z^j\ , \end{aligned} \tag{2.3}$$

where $\sigma_\pm^j$ and σ_z^j are pseudospin operators for the jth atom, satisfying commutation relations $[\sigma_+^j,\sigma_-^k]=2\sigma_z^j\delta_{jk}$ and $[\sigma_\pm^j,\sigma_z^k]=\mp\sigma_\pm^j\delta_{jk}$.

In OBII a Fokker-Planck equation has been derived to describe the coupled system of atoms plus cavity mode. Interactions with thermal reservoirs model radiative and collisional atomic decay and losses at the cavity mirrors. Using the positive P representation[5] (generalized to include atomic operators), the correspondence between c numbers and operators is

$$\vec{\xi}\equiv\begin{pmatrix} j_1\\ j_2\\ j_3\\ \alpha_1\\ \alpha_2\end{pmatrix}\leftrightarrow\begin{pmatrix} J_-\\ J_+\\ J_z\\ a\\ a^\dagger\end{pmatrix}\ , \tag{2.4}$$

where j_1, j_2, j_3, α_1, and α_2 are all independent complex variables and the Fokker-Planck equation reads[18]

$$\frac{\partial P}{\partial t}(\vec{\xi},t)=\left[-\sum_{\mu}\frac{\partial}{\partial \xi_\mu}A_{\xi_\mu}(\vec{\xi})+\frac{1}{2}\frac{\partial^2}{\partial\xi_\mu\partial\xi_\nu}D_{\xi_\mu,\xi_\nu}(\vec{\xi})\right]P(\vec{\xi},t) \tag{2.5}$$

with

$$A_{j_1}=-\gamma_\perp(1+i\delta)j_1+2gj_3\alpha_1\ ,$$
$$A_{j_2}=-\gamma_\perp(1-i\delta)j_2+2gj_3\alpha_2\ , \tag{2.6}$$
$$A_{j_3}=-\gamma_{\parallel}\left[j_3+\frac{N}{2}\right]-g(j_1\alpha_2+j_2\alpha_1)\ ,$$

$$A_{\alpha_1}=-\kappa(1+i\phi)\alpha_1+gj_1+\kappa\overline{\mathscr{E}}_i\ ,$$
$$A_{\alpha_2}=-\kappa(1-i\phi)\alpha_2+gj_2+\kappa\overline{\mathscr{E}}_i^*\ , \tag{2.7}$$

and

$$D_{j_1,j_1}=2gj_1\alpha_1\ ,$$
$$D_{j_2,j_2}=2gj_2\alpha_2\ ,$$
$$D_{j_3,j_3}=\gamma_{\parallel}\left[j_3+\frac{N}{2}\right]-g(j_1\alpha_2+j_2\alpha_1)\ , \tag{2.8}$$
$$D_{j_1,j_2}=D_{j_2,j_1}=(2\gamma_\perp-\gamma_{\parallel})\left[j_3+\frac{N}{2}\right]\ ,$$

all remaining D_{ξ_μ,ξ_ν} are zero. Here $\gamma_{\parallel}$ and $\gamma_\perp$ are longitudinal and transverse atomic relaxation rates,

$$\kappa=(1-R)c/(L+\hat{L}) \tag{2.9}$$

is the cavity relaxation rate,

$$g=(\omega_c\mu^2/2\hbar\epsilon_0V_Q)^{1/2} \tag{2.10}$$

is the atom-field coupling constant,

$$\delta=(\omega_a-\omega_0)/\gamma_\perp \tag{2.11}$$

and

$$\phi=(\omega_c-\omega_0)/\kappa \tag{2.12}$$

are atomic and cavity detunings, and

$$\overline{\mathscr{E}}_i=-i(2\epsilon_0V_Q/\hbar\omega_c)^{1/2}e^{i\phi_T}\mathscr{E}_i/(1-R)^{1/2}\ . \tag{2.13}$$

Apart from the fact that j_3 is complex and j_1,j_2 and α_1,α_2 are not complex-conjugate pairs, this formulation follows Haken's treatment for the laser.[4] Classical averages in the space of c numbers give normally ordered quantum averages,

$$\langle J_+^pJ_z^qJ_-^r a^{\dagger s}a^t\rangle=\int d^2\vec{\xi}\,P(\vec{\xi})j_2^pj_3^qj_1^r\alpha_2^s\alpha_1^t\ . \tag{2.14}$$

Throughout quantum averages $\langle\ \rangle$ are taken with respect to the rotating density operator

$$\rho_{\rm rot}(t)=\exp[i\omega_0(J_z+a^\dagger a)t]\times\rho(t)\exp[-i\omega_0(J_z+a^\dagger a)t]\ .$$

It is shown in OBII that Eq. (2.5) is equivalent to a Fokker-Planck equation with positive-semidefinite diffusion. There, atomic variables were adiabatically eliminated from the corresponding Îto stochastic differential equation. Here we follow the same methods, but rather adiabatically eliminate the field variables—in the "bad cavity" limit.[19] We have

$$\alpha_1=(1+i\phi)^{-1}\left[\overline{\mathscr{E}}_i+\frac{g}{\kappa}j_1\right]\ ,$$
$$\alpha_2=(1-i\phi)^{-1}\left[\overline{\mathscr{E}}_i^*+\frac{g}{\kappa}j_2\right]\ , \tag{2.15}$$

and the resulting equations for j_1, j_2, and j_3 are

$$\frac{dj_1}{dt}=-\gamma_\perp(1+i\delta)j_1+\frac{2g}{1+i\phi}j_3\left[\overline{\mathscr{E}}_i+\frac{g}{\kappa}j_1\right]+\Gamma_{j_1}\ ,$$
$$\frac{dj_2}{dt}=-\gamma_\perp(1-i\delta)j_2+\frac{2g}{1-i\phi}j_3\left[\overline{\mathscr{E}}_i^*+\frac{g}{\kappa}j_2\right]+\Gamma_{j_2}\ , \tag{2.16}$$
$$\frac{dj_3}{dt}=-\gamma_{\parallel}\left[j_3+\frac{N}{2}\right]-g\left[\frac{\overline{\mathscr{E}}_i^*}{1-i\phi}j_1+\frac{\overline{\mathscr{E}}_i}{1+i\phi}j_2\right]-\frac{2g^2}{\kappa(1+\phi^2)}j_1j_2+\Gamma_{j_3}\ ,$$

where Γ_{j_1}, Γ_{j_2}, and Γ_{j_3} are Gaussian random variables with

$$\begin{aligned}
\langle \Gamma_{j_1}(t)\Gamma_{j_1}(t')\rangle &= \frac{2g}{1+i\phi} j_1 \left[\overline{\mathscr{E}}_i + \frac{g}{\kappa} j_1 \right] \delta(t-t') , \\
\langle \Gamma_{j_2}(t)\Gamma_{j_2}(t')\rangle &= \frac{2g}{1-i\phi} j_2 \left[\overline{\mathscr{E}}_i^* + \frac{g}{\kappa} j_2 \right] \delta(t-t') , \\
\langle \Gamma_{j_3}(t)\Gamma_{j_3}(t')\rangle &= \left[\gamma_{\parallel} \left[j_3 + \frac{N}{2} \right] - g \left[\frac{\overline{\mathscr{E}}_i^*}{1-i\phi} j_1 + \frac{\overline{\mathscr{E}}_i}{1+i\phi} j_2 \right] - \frac{2g^2}{\kappa(1+\phi^2)} j_1 j_2 \right] \delta(t-t') , \\
\langle \Gamma_{j_1}(t)\Gamma_{j_2}(t')\rangle &= \langle \Gamma_{j_2}(t)\Gamma_{j_1}(t')\rangle = (2\gamma_{\perp} - \gamma_{\parallel}) \left[j_3 + \frac{N}{2} \right] \delta(t-t') ,
\end{aligned} \tag{2.17}$$

and all remaining correlations are zero.

The steady-state mean-field theory for optical bistability in a ring cavity[20] follows from solutions to Eqs. (2.16) with the time derivatives and Gaussian noise sources set to zero. The basis for our linearized theory of fluctuations is a Fokker-Planck equation corresponding to the Langevin equations obtained after linearizing Eqs. (2.16) about this steady state and substituting steady-state solutions j_1^{ss}, j_2^{ss}, and j_3^{ss} into Eqs. (2.17). We define a scaled time $\tau = \gamma_{\perp} t$ and new variables

$$\vec{\tilde{\mathrm{j}}} \equiv \begin{bmatrix} \tilde{j}_1 \\ \tilde{j}_2 \\ \tilde{j}_3 \end{bmatrix} = \frac{1}{N} \begin{bmatrix} j_1 - j_1^{ss} \\ j_2 - j_2^{ss} \\ j_3 - j_3^{ss} \end{bmatrix} ; \quad \vec{\tilde{\mathrm{j}}}' = \begin{bmatrix} \partial/\partial \tilde{j}_1 \\ \partial/\partial \tilde{j}_2 \\ \partial/\partial \tilde{j}_3 \end{bmatrix} . \tag{2.18}$$

The Fokker-Planck equation reads

$$\frac{\partial P}{\partial \tau}(\vec{\tilde{\mathrm{j}}},\tau) = \left[\vec{\tilde{\mathrm{j}}}'^{T} A \vec{\tilde{\mathrm{j}}} + \frac{1}{2N} \vec{\tilde{\mathrm{j}}}'^{T} D \vec{\tilde{\mathrm{j}}}' \right] P(\vec{\tilde{\mathrm{j}}},\tau) , \tag{2.19}$$

where

$$A = \begin{bmatrix} a & 0 & b \\ 0 & a^* & b^* \\ c & c^* & d \end{bmatrix} , \tag{2.20}$$

$$D = \begin{bmatrix} e & f & 0 \\ f & e^* & 0 \\ 0 & 0 & g \end{bmatrix} , \tag{2.21}$$

with

$$\begin{aligned}
a &= \frac{1+i\delta}{1+i\phi} \frac{Y}{X} e^{i(\phi_y - \phi_x)} , \\
b &= i\sqrt{2\Gamma} X e^{i\phi_x} , \\
c &= i\sqrt{\Gamma/2} X e^{-i\phi_x} \left[1 - \frac{1+i\delta}{1+i\phi} \frac{2C}{1+\delta^2+X^2} \right] , \\
d &= 2\Gamma ,
\end{aligned} \tag{2.22}$$

and

$$\begin{aligned}
e &= \Gamma(1-i\delta) e^{2i\phi_x} X^2/(1+\delta^2+X^2) , \\
f &= (1-\Gamma) X^2/(1+\delta^2+X^2) , \\
g &= 2\Gamma X^2/(1+\delta^2+X^2) .
\end{aligned} \tag{2.23}$$

We have defined

$$\Gamma = \gamma_{\parallel}/2\gamma_{\perp} , \tag{2.24}$$

$$C = Ng^2/2\kappa\gamma_{\perp} = \alpha L/4(1-R) , \tag{2.25}$$

where $\alpha = N\mu^2\omega_c/\epsilon_0\hbar V_I \gamma_{\perp} c$ is the resonant absorption coefficient and $Y\exp(i\phi_y)$ and $X\exp(i\phi_x)$ are the dimensionless driving field and mean cavity field amplitudes:

$$\begin{aligned}
Y e^{i\phi_y} &= i2g\overline{\mathscr{E}}_i/(\gamma_{\parallel}\gamma_{\perp})^{1/2} \\
&= (1-R)^{-1/2} \mathscr{E}_i/\mathscr{E}_s , \\
X e^{i\phi_x} &= 2g\langle a \rangle/(\gamma_{\parallel}\gamma_{\perp})^{1/2} \\
&= (1-R)^{-1/2} e^{-i\phi_T} \mathscr{E}_t/\mathscr{E}_s ,
\end{aligned} \tag{2.26}$$

where $\mathscr{E}_s = (\hbar/2\mu)(\gamma_{\parallel}\gamma_{\perp})^{1/2}$ is the saturation amplitude and $\mathscr{E}_t$ is the transmitted field amplitude. For given C, δ, ϕ, and $Y\exp(i\phi_y)$, the complex amplitude $X\exp(i\phi_x)$ satisfies the state equation[20]

$$Y e^{i\phi_y} = X e^{i\phi_x} \left[(1+i\phi) + (1-i\delta) \frac{2C}{1+\delta^2+X^2} \right] . \tag{2.27}$$

III. STEADY-STATE CORRELATIONS

In Eq. (2.19), $\tilde{j}_1$, $\tilde{j}_2$, and $\tilde{j}_3$ are independent complex variables. It can be shown that the restrictions $\tilde{j}_3 = \tilde{j}_3^*$, $\tilde{j}_1 = \tilde{j}_2^*$—as in Haken's laser theory[4]—lead to a Fokker-Planck equation with nonpositive-definite diffusion. Using the positive P representation, Eq. (2.19) is interpreted within a six-dimensional space where, defining $\overset{\rightleftarrows}{\mathrm{j}}_x$, $\overset{\rightleftarrows}{\mathrm{j}}_y$, $\overset{\rightleftarrows}{\mathrm{j}}{}'_x$, and $\overset{\rightleftarrows}{\mathrm{j}}{}'_y$ by

$$\begin{aligned}\overset{\rightleftarrows}{\mathrm{j}} &= \overset{\rightleftarrows}{\mathrm{j}}_x + i\,\overset{\rightleftarrows}{\mathrm{j}}_y\;,\\ \overset{\rightleftarrows}{\mathrm{j}}{}' &= \tfrac{1}{2}(\overset{\rightleftarrows}{\mathrm{j}}{}'_x - i\,\overset{\rightleftarrows}{\mathrm{j}}{}'_y)\;,\end{aligned} \tag{3.1}$$

it is shown to be equivalent to[1,5]

$$\begin{aligned}\frac{\partial P}{\partial\tau}(\overset{\rightleftarrows}{\mathrm{j}}_x,\overset{\rightleftarrows}{\mathrm{j}}_y,\tau) = \Bigg[&\begin{bmatrix}\overset{\rightleftarrows}{\mathrm{j}}{}'_x\\ \overset{\rightleftarrows}{\mathrm{j}}{}'_y\end{bmatrix}^T \hat{A} \begin{bmatrix}\overset{\rightleftarrows}{\mathrm{j}}_x\\ \overset{\rightleftarrows}{\mathrm{j}}_y\end{bmatrix}\\ &+\frac{1}{2N}\begin{bmatrix}\overset{\rightleftarrows}{\mathrm{j}}{}'_x\\ \overset{\rightleftarrows}{\mathrm{j}}{}'_y\end{bmatrix}^T \hat{D} \begin{bmatrix}\overset{\rightleftarrows}{\mathrm{j}}{}'_x\\ \overset{\rightleftarrows}{\mathrm{j}}{}'_y\end{bmatrix}\Bigg]\\ &\times P(\overset{\rightleftarrows}{\mathrm{j}}_x,\overset{\rightleftarrows}{\mathrm{j}}_y,\tau)\end{aligned} \tag{3.2}$$

with

$$\begin{aligned}\hat{A} &= \begin{bmatrix}A^x & -A^y\\ A^y & A^x\end{bmatrix},\\ A &= A^x + iA^y\;,\end{aligned} \tag{3.3}$$

$$\begin{aligned}\hat{D} &= \begin{bmatrix}B^x B^{x^T} & B^x B^{y^T}\\ B^y B^{x^T} & B^y B^{y^T}\end{bmatrix},\\ D &= (B^x + iB^y)(B^x + iB^y)^T\;.\end{aligned} \tag{3.4}$$

This equation has an explicitly positive-semidefinite diffusion.

The solution to Eq. (3.2) is a Gaussian in six dimensions and the steady-state correlation matrix

$$\hat{G} = \begin{bmatrix}G^{xx} & G^{xy}\\ G^{yx} & G^{yy}\end{bmatrix},\quad G^{\mu\nu} = \mathrm{av}(\overset{\rightleftarrows}{\mathrm{j}}_\mu \overset{\rightleftarrows}{\mathrm{j}}{}_\nu^T)_{\mathrm{ss}}\;, \tag{3.5}$$

satisfies the equation[21]

$$\hat{A}\hat{G} + \hat{G}\hat{A}^T = \frac{1}{N}\hat{D}\;. \tag{3.6}$$

We use av( )$_{\mathrm{ss}}$ to denote classical steady-state averages. We are only interested in physical correlations, however; namely, those corresponding to normally ordered quantum averages [Eq. (2.14)]. We restrict our attention to the physical correlation matrix

$$G = \mathrm{av}(\overset{\rightleftarrows}{\mathrm{j}}\,\overset{\rightleftarrows}{\mathrm{j}}{}^T)_{\mathrm{ss}} = (G^{xx} - G^{yy}) + i(G^{xy} + G^{yx})\;. \tag{3.7}$$

From Eqs. (3.3)–(3.7) it can be shown that G satisfies the matrix equation

$$AG + GA^T = \frac{1}{N}D\;. \tag{3.8}$$

This is precisely the equation we would obtain by strictly following Haken's treatment for the laser—to Eq. (2.19) with $\tilde{j}_3 = \tilde{j}_3^*$, $\tilde{j}_1 = \tilde{i}_?^*$—and naively overlooking the fact that represents a nonpositive-definite diffusior

To solve Eq. (3.8) we write

$$G = \begin{bmatrix}u & w & v\\ w & u^* & v^*\\ v & v^* & z\end{bmatrix}, \tag{3.9}$$

where

$$\begin{aligned}u &= \mathrm{av}(\tilde{j}_1\tilde{j}_1)_{\mathrm{ss}} = \langle \tilde{J}_-\tilde{J}_-\rangle_{\mathrm{ss}}\;,\\ v &= \mathrm{av}(\tilde{j}_3\tilde{j}_1)_{\mathrm{ss}} = \langle \tilde{J}_z\tilde{J}_-\rangle_{\mathrm{ss}}\;,\\ w &= \mathrm{av}(\tilde{j}_2\tilde{j}_1)_{\mathrm{ss}} = \langle \tilde{J}_+\tilde{J}_-\rangle_{\mathrm{ss}}\;,\\ z &= \mathrm{av}(\tilde{j}_3\tilde{j}_3)_{\mathrm{ss}} = \langle \tilde{J}_z\tilde{J}_z\rangle_{\mathrm{ss}}\end{aligned} \tag{3.10}$$

with

$$\begin{aligned}\tilde{J}_\pm &= \frac{1}{N}(J_\pm - \langle J_\pm\rangle_{\mathrm{ss}})\;,\\ \tilde{J}_z &= \frac{1}{N}(J_z - \langle J_z\rangle_{\mathrm{ss}})\;.\end{aligned} \tag{3.11}$$

Equation (3.8) then corresponds to the following set of coupled matrix equations:

$$\begin{aligned}&\begin{bmatrix}a & 0\\ 0 & a^*\end{bmatrix}\begin{bmatrix}u\\ u^*\end{bmatrix} + \begin{bmatrix}b & 0\\ 0 & b^*\end{bmatrix}\begin{bmatrix}v\\ v^*\end{bmatrix} = \frac{1}{2N}\begin{bmatrix}e\\ e^*\end{bmatrix},\\ &\begin{bmatrix}c & 0\\ 0 & c^*\end{bmatrix}\begin{bmatrix}u\\ u^*\end{bmatrix} + \begin{bmatrix}a+d & 0\\ 0 & a^*+d\end{bmatrix}\begin{bmatrix}v\\ v^*\end{bmatrix}\\ &\qquad + \begin{bmatrix}c^* & b\\ c & b^*\end{bmatrix}\begin{bmatrix}w\\ z\end{bmatrix} = 0\;, \qquad (3.12)\\ &\begin{bmatrix}b^* & b\\ c & c^*\end{bmatrix}\begin{bmatrix}v\\ v^*\end{bmatrix} + \begin{bmatrix}a+a^* & 0\\ 0 & d\end{bmatrix}\begin{bmatrix}w\\ z\end{bmatrix} = \frac{1}{2N}\begin{bmatrix}2f\\ g\end{bmatrix}.\end{aligned}$$

Solving this set of equations is a straightforward exercise. We find

$$\langle \tilde{J}_z\tilde{J}_-\rangle_{\mathrm{ss}} = \frac{1}{2N}(PR^* + QR)/(\,|P|^2 - |Q|^2)\;, \tag{3.13}$$

where

$$\begin{aligned}P &= bc^*\left[\frac{1}{a+a^*} + \frac{1}{d}\right],\\ Q &= (a^*+d)\left[1 - \frac{b^*c^*}{a^*d}\right] - \frac{bc}{a+a^*}\;,\\ R &= \frac{c}{a}e + \frac{2c^*}{a+a^*}f + \frac{b}{d}g\;,\end{aligned} \tag{3.14}$$

and

$$\langle \tilde{J}_-\tilde{J}_- \rangle_{ss} = \frac{1}{2N}[e - b(2N\langle \tilde{J}_z\tilde{J}_- \rangle_{ss})]/a \; , \qquad (3.15)$$

$$\langle \tilde{J}_+\tilde{J}_- \rangle_{ss} = \frac{1}{2N}\mathrm{Re}[f - b^*(2N\langle \tilde{J}_z\tilde{J}_- \rangle_{ss})]/\mathrm{Re}(a) \; , \qquad (3.16)$$

$$\langle \tilde{J}_z\tilde{J}_z \rangle_{ss} = \frac{1}{2N}\mathrm{Re}[g - 2c(2N\langle \tilde{J}_z\tilde{J}_- \rangle_{ss})]/d \; . \qquad (3.17)$$

For absorptive bistability ($\delta = \phi = 0$) we have checked Eqs. (3.13), (3.15), and (3.16) against Lugiato's results [Eqs. (5.12a), (5.12b), and (5.12c) in Ref. 7] and find perfect agreement. For $\Gamma = 1$—purely radiative atomic damping—our results also agree with those of Agarwal *et al.*[6] This agreement provides explicit verification of our use of the positive P representation to justify Eq. (3.8) with its implied neglect of a nonpositive-definite diffusion.

Amongst the various steady-state correlations the result of most physical interest is that for $\langle \tilde{J}_+\tilde{J}_- \rangle_{ss}$. This gives the incoherent transmitted intensity. With the full transmitted intensity divided into coherent and incoherent contributions we have

$$I_t^{ss} = T_{coh}^{ss} + T_{inc}^{ss} \; ,$$

$$T_{coh}^{ss}/\mathscr{E}_s^2(1-R) = X^2 \; , \qquad (3.18)$$

$$T_{inc}^{ss}/\mathscr{E}_s^2(1-R) = \frac{1}{N\Gamma}\left[\frac{4C^2}{(1+\phi^2)}\right](2N\langle \tilde{J}_+\tilde{J}_- \rangle_{ss}) \; .$$

We have plotted the ratio $N\Gamma T_{inc}^{ss}/T_{coh}^{ss}$ in Fig. 1 for $C = 20$, $\delta = 1$, $\phi = -2$, and various values of Γ. These parameters give bistability, and the behavior for other parameters satisfying the bistability conditions

$$4(C + \delta\phi - 1)^3 \geq 27C(1+\delta^2)(1+\phi^2) \; , \qquad 2C > \delta\phi - 1 \; , \qquad (3.19)$$

are similar. The divergences in Fig. 1 occur at the turning points, $dY/dX = 0$, of the S-shaped bistability curve (see Ref. 20) plotted from Eq. (2.27). Here the linearization introduced in Sec. II breaks down; the steady state is no longer locally stable. As Γ decreases, corresponding to an increase in phase destroying atomic collisions, the divergences are narrowed. Note that as $\Gamma \to 0$, along the lower branch [Fig. 1(a)], $N\Gamma T_{inc}^{ss}/T_{coh}^{ss}$ develops a local minimum,

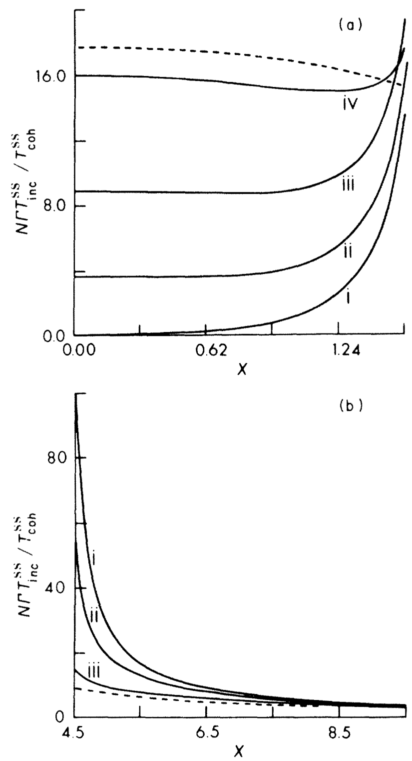

FIG. 1. The ratio of incoherent and coherent transmitted intensities for $C = 20$, $\delta = 1.0$, and $\phi = -2.0$. Turning points in the bistability curve are at $X = 1.71$, $Y = 23.3$ and $X = 4.30$, $Y = 21.2$. (a) Lower branch with (i) $\Gamma = 1.00$, (ii) $\Gamma = 0.80$, (iii) $\Gamma = 0.50$, and (iv) $\Gamma = 0.10$. (b) Upper branch with (i) $\Gamma = 1.00$, (ii) $\Gamma = 0.10$, and (iii) $\Gamma = 0.01$. The dashed curves are for the limit $\Gamma \to 0$ [Eq. (3.20)].

and in the limit

$$N\Gamma T_{inc}^{ss}/T_{coh}^{ss} = 4C^2/[(1+\phi^2)X^2 + (1+\delta^2)(1+\phi^2+2C)] \; . \qquad (3.20)$$

This is a monotonically decreasing function of X; the divergences now have zero width.

IV. TRANSMITTED SPECTRUM

The argument used to justify Eq. (3.8) applies in a similar fashion to a calculation of the spectrum of fluctuations. In the six-dimensional $(\vec{j}_x, \vec{j}_y)$ space we define

$$\hat{G}(\tau) = \begin{bmatrix} G^{xx}(\tau) & G^{xy}(\tau) \\ G^{yx}(\tau) & G^{yy}(\tau) \end{bmatrix} ,$$

$$G^{\mu\nu}(\tau) = \mathrm{av}(\vec{j}_\mu(\tau)\,\vec{j}_\nu^{\,T})_{ss} \; , \qquad (4.1)$$

and the corresponding spectrum

$$\hat{C}(\bar{\omega})=\frac{1}{2\pi}\int_{-\infty}^{\infty}d\tau\, e^{-i\bar{\omega}\tau}\hat{G}(\tau) \tag{4.2}$$

is given by[21]

$$\hat{C}(\bar{\omega})=\frac{1}{2\pi N}(\hat{A}-i\bar{\omega}I_6)^{-1}\hat{D}(\hat{A}^T+i\bar{\omega}I_6)^{-1}\ , \tag{4.3}$$

where I_6 is the 6×6 identity matrix. We use $\bar{\omega}$ to indicate a dimensionless frequency complementary to the dimensionless time τ. Then, in like manner to the relationship between Eqs. (3.6) and (3.8), with

$$G(\tau)=\mathrm{av}(\vec{j}(\tau)\vec{j}^{\,T})_{\mathrm{ss}}=[G^{xx}(\tau)-G^{yy}(\tau)] +i[G^{xy}(\tau)+G^{yx}(\tau)]\ , \tag{4.4}$$

from Eq. (4.3) it can be shown that

$$\begin{aligned} C(\bar{\omega})&=\frac{1}{2\pi}\int_{-\infty}^{\infty}d\tau\, e^{-i\bar{\omega}\tau}G(\tau)\\ &=\frac{1}{2\pi N}(A-i\bar{\omega}I_3)^{-1}D(A^T+i\bar{\omega}I_3)^{-1}\ , \end{aligned} \tag{4.5}$$

where I_3 is the 3×3 identity matrix. This is again precisely the equation we would obtain from Eq. (2.19) if, with $\tilde{j}_3=\tilde{j}_3^{\,*}$, $\tilde{j}_1=\tilde{j}_2^{\,*}$, we naively overlook the fact that D represents a nonpositive-definite diffusion.[22]

Corresponding to the separation of coherent and incoherent intensities in Eq. (3.18), the spectrum of the transmitted light is written

$$T_{\mathrm{ss}}(\bar{\omega})=T_{\mathrm{coh}}^{\mathrm{ss}}\delta(\bar{\omega})+T_{\mathrm{inc}}^{\mathrm{ss}}\mathscr{F}(\bar{\omega})\ , \tag{4.6}$$

where[7]

$$\begin{aligned}\mathscr{F}(\bar{\omega})&=\langle\tilde{J}_+\tilde{J}_-\rangle_{\mathrm{ss}}^{-1}\frac{1}{2\pi}\int_{-\infty}^{\infty}d\tau\, e^{-i\bar{\omega}\tau}\langle\tilde{J}_+(\tau)\tilde{J}_-\rangle_{\mathrm{ss}}\\ &=\langle\tilde{J}_+\tilde{J}_-\rangle_{\mathrm{ss}}^{-1}\frac{1}{2\pi}\int_{-\infty}^{\infty}d\tau\, e^{-i\bar{\omega}\tau}\mathrm{av}(\tilde{j}_2(\tau)\tilde{j}_1)_{\mathrm{ss}}\\ &=\langle\tilde{J}_+\tilde{J}_-\rangle_{\mathrm{ss}}^{-1}C(\bar{\omega})_{21}\ ,\end{aligned} \tag{4.7}$$

and from Eq. (4.5) we find

$$C(\bar{\omega})_{21}=\frac{1}{2\pi N}|\Lambda(i\bar{\omega})|^{-2}\mathrm{Re}\{2bc^*e^*[(a+i\bar{\omega})(d+i\bar{\omega})-bc] +f[|(a+i\bar{\omega})(d+i\bar{\omega})-bc|^2+|bc|^2]+g|b(a+i\bar{\omega})|^2\} \tag{4.8}$$

with

$$\Lambda(i\bar{\omega})=(a-i\bar{\omega})(a^*-i\bar{\omega})(d-i\bar{\omega})-bc(a^*-i\bar{\omega})-b^*c^*(a-i\bar{\omega})\ . \tag{4.9}$$

Here the spectrum is normalized with respect to the dimensionless frequency $\bar{\omega}$,

$$\int_{-\infty}^{\infty}d\bar{\omega}\,\mathscr{F}(\bar{\omega})=1\ ,\quad \int_{-\infty}^{\infty}d\bar{\omega}\,T_{\mathrm{ss}}(\bar{\omega})=T_{\mathrm{coh}}^{\mathrm{ss}}+T_{\mathrm{inc}}^{\mathrm{ss}}\ .$$

As a function of the dimensioned optical frequency ω, the normalized spectrum is given by $\gamma_\perp^{-1}T_{\mathrm{ss}}(\bar{\omega})$ with $\bar{\omega}=(\omega-\omega_0)/\gamma_\perp$.

In principle, the incoherent spectrum $\mathscr{F}(\bar{\omega})$ can be decomposed into the sum of three Lorentzian components with

$$C(\bar{\omega})_{21}=\frac{1}{2\pi N}\sum_{\mu=1}^{3}\frac{\alpha_\mu[\bar{\omega}-\mathrm{Im}(\lambda_\mu)]+\beta_\mu}{[\bar{\omega}-\mathrm{Im}(\lambda_\mu)]^2+[\mathrm{Re}(\lambda_\mu)]^2}\ , \tag{4.10}$$

where the λ_μ are roots of the cubic equation $\Lambda(\lambda)=0$, and α_μ and β_μ are real coefficients. For absorptive bistability ($\delta=\phi=0$) we have obtained $\mathscr{F}(\bar{\omega})$ in this form and compared our results with the work of Lugiato,[7] and, for $\Gamma=1$, with the work of Agarwal *et al.*[6] Our results agree, a further explicit confirmation of our methods. With nonzero atomic and cavity detunings this decomposition is generally not practicable. However, it can be made for the weak-field limit $X^2\ll 1+\delta^2$:

$$\lambda_1=\lambda_2^*=a=\left[1+\frac{2C}{1+\phi^2}\right]+i\left[\delta-\phi\frac{2C}{1+\phi^2}\right],\qquad \lambda_3=d=2\Gamma\,, \tag{4.11}$$

and

$$\begin{aligned}\alpha_1&=-\alpha_2=-\frac{1}{2}\frac{X^2}{1+\delta^2}\Gamma X^2|a|^{-2}\mathrm{Re}(a)/\mathrm{Im}(a)\,,\\ \beta_1&=\frac{X}{1+\delta^2}[(1-\Gamma)+\tfrac{1}{2}\Gamma X^2|a|^{-2}\mathrm{Re}(a)]\,,\\ \beta_2&=\frac{1}{2}\frac{X^2}{1+\delta^2}\Gamma X^2|a|^{-2}\mathrm{Re}(a)\,,\\ \alpha_3&=\beta_3=0\,,\end{aligned} \tag{4.12}$$

with

$$\begin{aligned}\langle\tilde J_+\tilde J_-\rangle_{ss}&=\int_{-\infty}^{\infty}d\bar\omega\, C(\bar\omega)_{21}\\ &=\frac{1}{2N}\frac{X^2}{1+\delta^2}[(1-\Gamma)+\Gamma X^2|a|^{-2}\mathrm{Re}(a)]/\mathrm{Re}(a)\,.\end{aligned} \tag{4.13}$$

Note the two types of terms appearing in Eqs. (4.12) and (4.13), terms in $(1-\Gamma)X^2/(1+\delta^2)$ and $\Gamma X^4/(1+\delta^2)$. Both must be retained. For $(1-\Gamma)\sim 1 \gg X^2$ the former is of dominant order, while for $(1-\Gamma)\ll X^2 \ll 1$ the latter is of dominant order [see feature 2(c) below]. We have dropped terms in $(1-\Gamma)X^4/(1+\delta^2)$ which are always of second order.

For absorptive bistability there has been much interest in collective features in the transmitted spectrum,[6,7,14,15] features such as (Fig. 2).

(1) Linewidth narrowing at the instabilities—turning points $dY/dX=0$ in bistability curves Y vs X.

(2) A spectral component with a broad cooperative linewidth along the lower branch.

(3) Premature merging of the Stark sidebands[16] along the upper branch, with the sidebands becoming higher than the central peak.

For various sets of parameters satisfying the bistability conditions [Eqs. (3.19)] $\mathscr{F}(\bar\omega)$ is plotted throughout the bistable region in Figs. 2–7. Here, corresponding collective features are illustrated for dispersive bistability.

(1) It may be shown that

$$|a|^2d-2\,\mathrm{Re}(bca^*)=\frac{Y}{X}\frac{dY}{dX}2\Gamma(1+\delta^2+X^2)(1+\phi^2)^{-1}\,. \tag{4.14}$$

Then the linewidth of one spectral component vanishes at each turning point, since, with $dY/dX=0$, the cubic equation $\Lambda(\lambda)=0$ [Eq. (4.9)] has a root $\lambda=0$. We find linewidth narrowing occurs as in absorptive bistability; Figs. 2–5 illustrate this on both the upper and lower branches. Only the beginning of the process is shown. In each example a close enough approach to the instability concentrates the entire spectral density in a single central peak with narrowing linewidth.

(2) A broad spectral component is present along the lower branch in dispersive bistability (Figs. 2–5). However various new features distinguish this case.

(a) The cooperative linewidth is modified by the cavity detuning in the manner indicated by Eqs. (4.11). The factor $(1+\phi^2)^{-1}$ expresses the effect of cavity detuning on the enhancement of the collective radiation reaction field by the cavity. It originates in the terms $(1\pm i\phi)^{-1}(g/\kappa)j_{1,2}$ in Eqs. (2.15), which contribute to the decay of fluctuations in the collective polarization via nonlinear terms in Eqs. (2.16).

(b) The broad component along the lower branch is generally a doublet associated with complex-conjugate roots to the cubic equation $\Lambda(\lambda)=0$; λ_1, and λ_2 in Eqs. (4.11). This is well illustrated in Figs. 3(a) and 5(a), while in Fig. 4(a) the doublet is not resolved, as the splitting is less than the broadened linewidth. For $\phi=0$ in Eqs. (4.11) the splitting by $\pm\delta$ corresponds to that in ordinary resonance fluorescence with a detuned driving field.[23] The

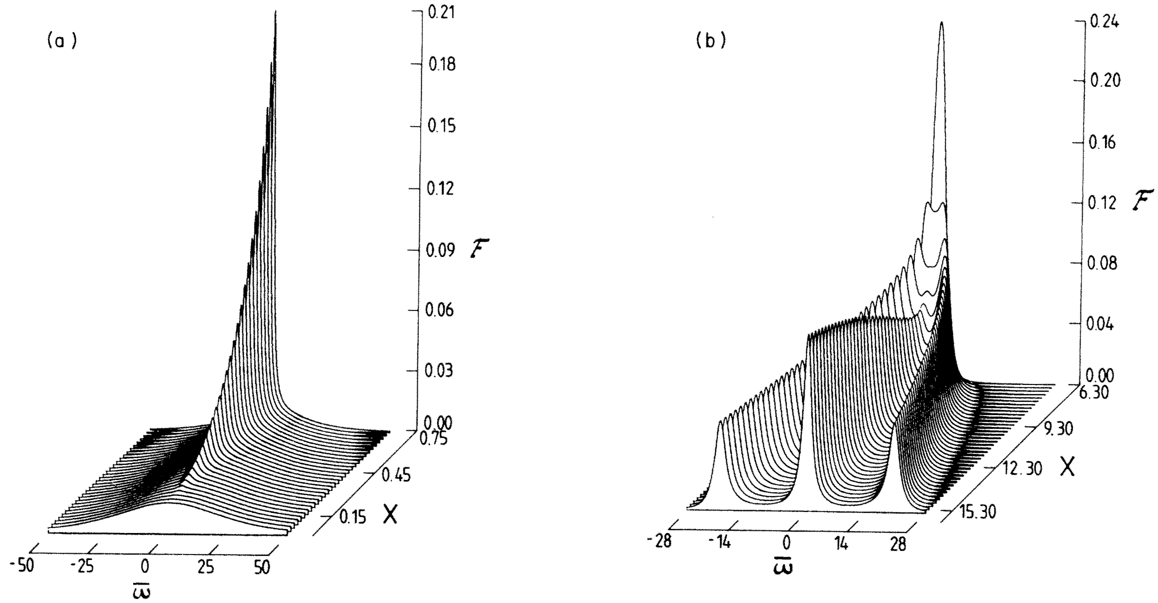

FIG. 2. The incoherent part of the transmitted spectrum for $C=20$, $\delta=0.0$, $\phi=0.0$, and $\Gamma=1.00$. Turning points in the bistability curve are at $X=1.05$, $Y=21.0$ and $X=6.07$, $Y=12.5$. (a) Lower branch, (b) upper branch.

contribution proportional to ϕ is due to the detuning between the collective polarization and the cavity, and the corresponding phase shift in the collective radiation reaction field [Eqs. (2.15) and (2.16)]. Note that in Figs. 3, 4, and 5 the broad spectral component remains as a doublet along the entire lower branch. At each turning point the cubic $\Lambda(\lambda)=0$ has one root $\lambda_3=0$, as note above, and two further roots

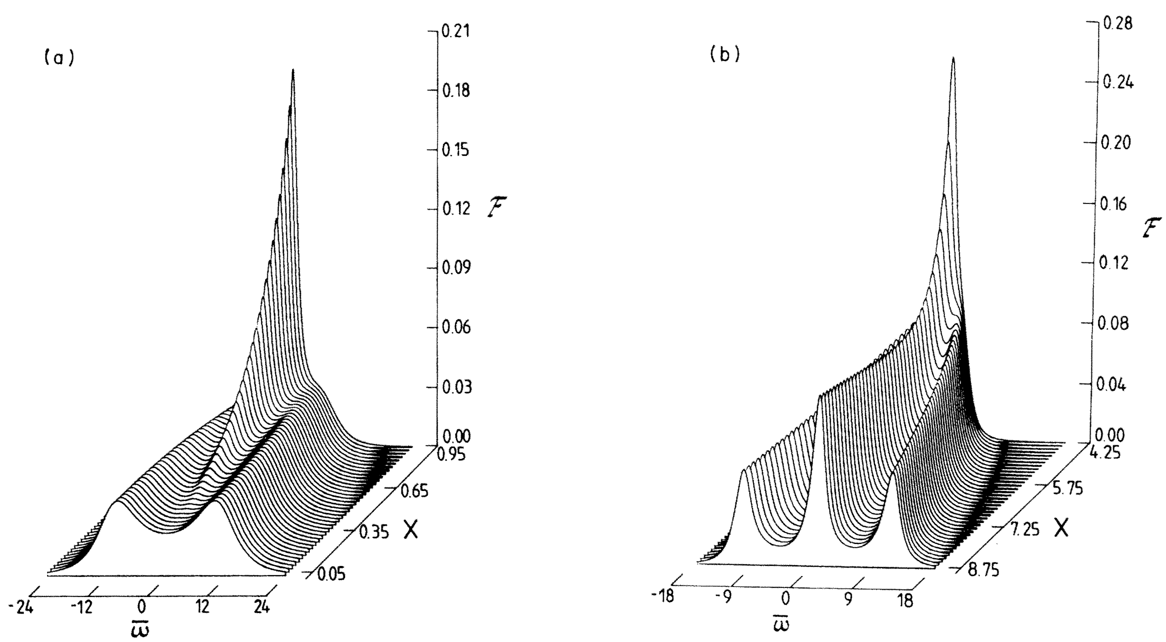

FIG. 3. The incoherent part of the transmitted spectrum ror $C=20$, $\delta=1.0$, $\phi=3.0$, and $\Gamma=1.00$. Turning points in the bistability curve are at $X=1.34$, $Y=18.5$ and $X=3.82$, $Y=13.2$. (a) Lower branch, (b) upper branch.

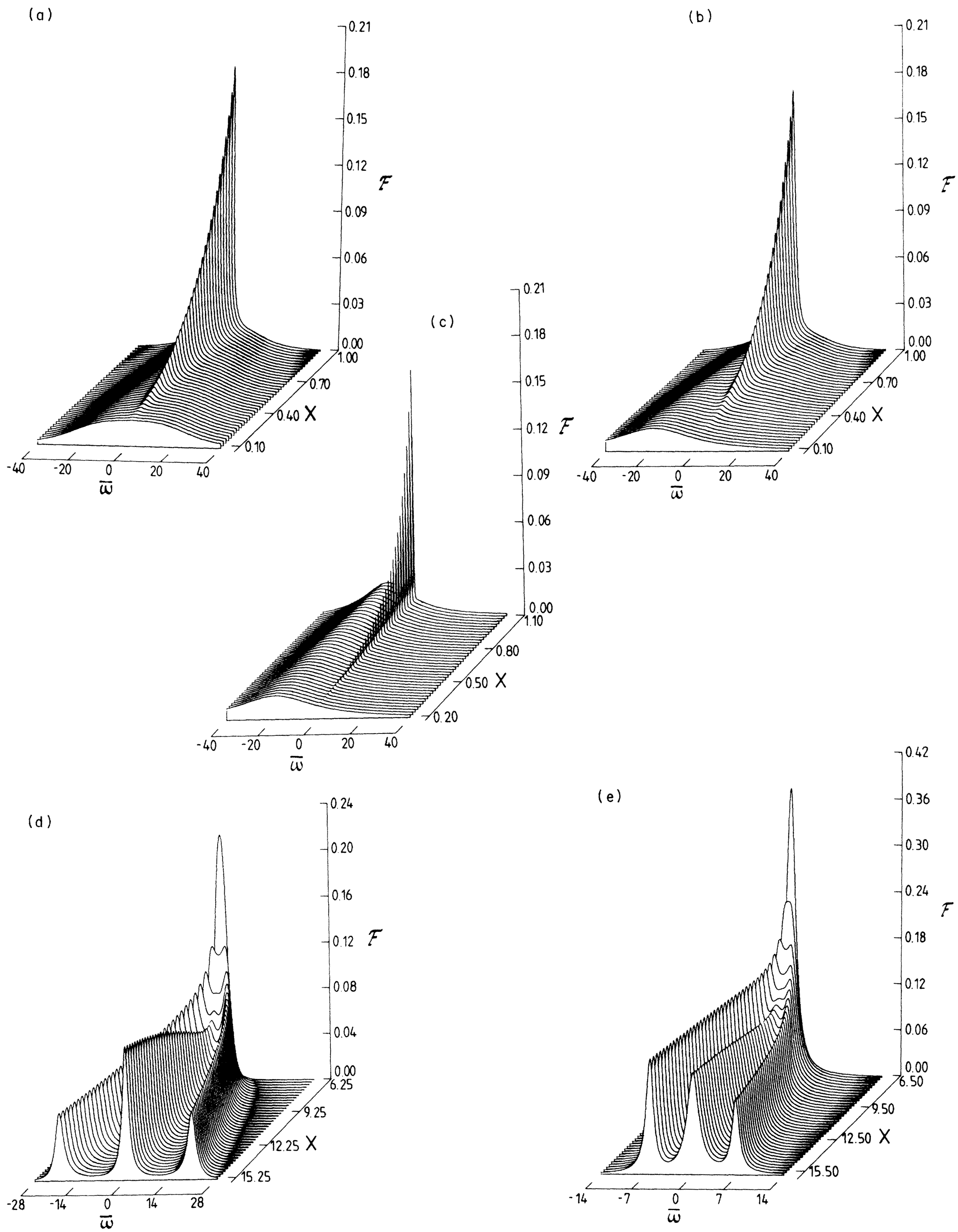

FIG. 4. The incoherent part of the transmitted spectrum for $C=20$ and $\delta=\phi=1.0$. Turning points in the bistability curve are at $X=1.43$, $Y=20.1$ and $X=5.99$, $Y=12.3$. (a) Lower branch, $\Gamma=1.00$; (b) lower branch, $\Gamma=0.99$; (c) lower branch, $\Gamma=0.10$; (d) upper branch $\Gamma=1.00$; (e) upper branch, $\Gamma=0.10$, where for clarity we use $\delta=\phi=-1.0$.

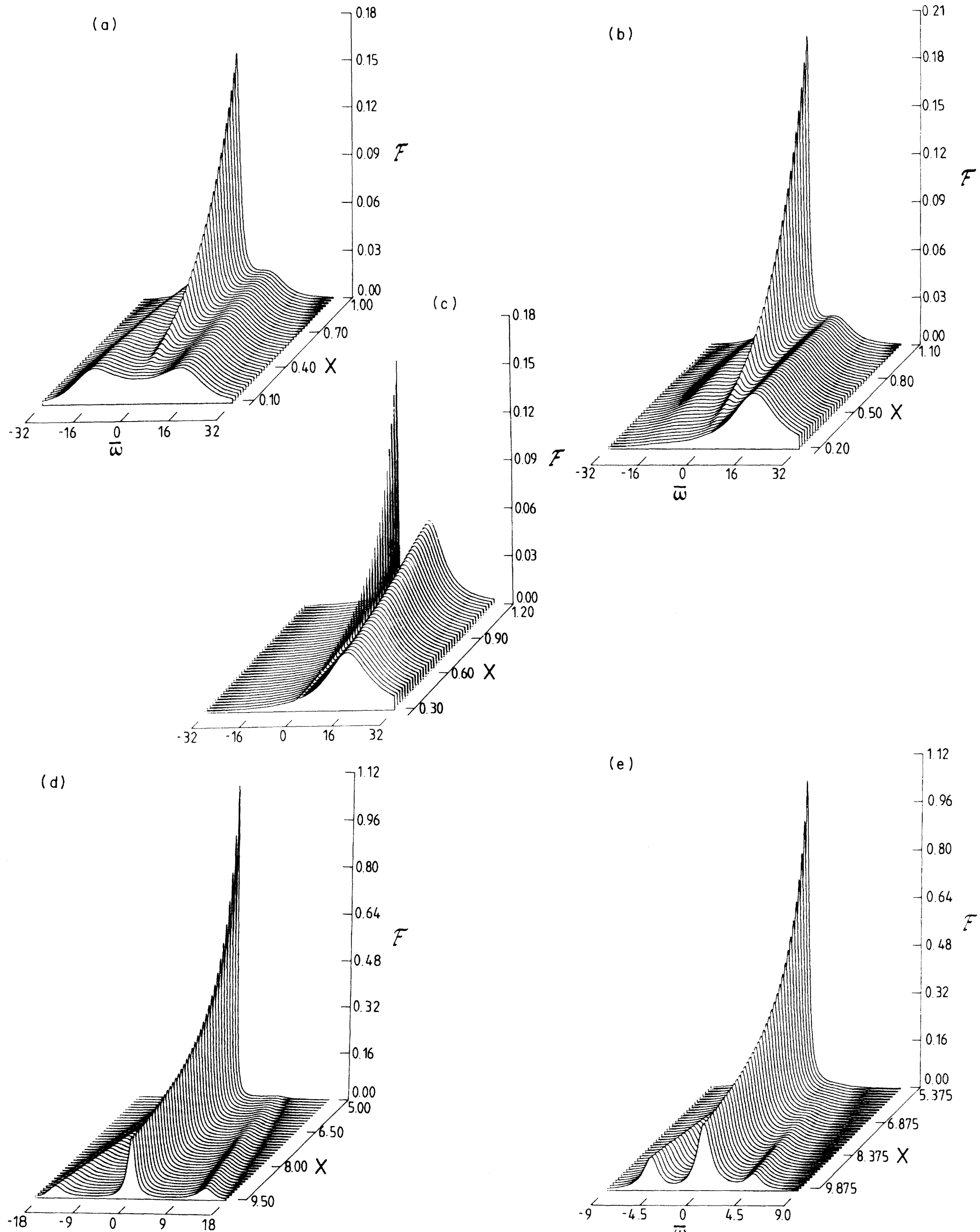

FIG. 5. The incoherent part of the transmitted spectrum for $C=20$, $\delta=1.0$, and $\phi=-2.0$. Turning points in the bistability curve are at $X=1.71$, $Y=23.3$ and $X=4.30$, $Y=21.2$. (a) Lower branch, $\Gamma=1.00$; (b) lower branch, $\Gamma=0.99$; (c) lower branch, $\Gamma=0.10$; (d) upper branch, $\Gamma=1.00$; (e) upper branch, $\Gamma=0.10$, where for clarity we use $\delta=-1.0$, $\phi=2.0$.

$$\lambda_{1,2}=\Gamma+\left[1+\frac{1+\delta^2}{1+\phi^2}\frac{2C}{1+\delta^2+X^2}\right]$$
$$\pm\left\{\Gamma^2-2\Gamma\left[\left[1+\frac{1+\delta^2}{1+\phi^2}\frac{2C}{1+\delta^2+X^2}\right]\right.\right.$$
$$\left.\left.+X^2\left[1-\frac{1+\delta\phi}{1+\phi^2}\frac{2C}{1+\delta^2+X^2}\right]\right]-\left[\delta-\phi\frac{1+\delta^2}{1+\phi^2}\frac{2C}{1+\delta^2+X^2}\right]^2\right\}^{1/2}. \tag{4.15}$$

At the turning point along the lower branch in Figs. 3(a), 4(a), and 5(a) we find $\lambda_{1,2}=4.11\mp i4.70$, $11.90\mp i7.98$, and $5.25\pm i8.89$, respectively.

(c) The broad doublet shows a sensitive dependence on dephasing atomic collisions. For purely radiative atomic decay ($\Gamma=1$), Figs. 3(a), 4(a), and 5(a) are symmetric about $\bar{\omega}=0$. With a 1% change in Γ a dramatic asymmetry is introduced in Figs. 4(b) and 5(b). At weak fields this asymmetry is little changed in Figs. 4(c) and 5(c) where Γ has been reduced by 90%. This behavior can be understood from Eqs. (4.12); β_1 differs from β_2 by a term $(1-\Gamma)X^2/(1+\delta^2)$. This term vanishes identically when $\Gamma=1$, but it dominates the spectrum when $(1-\Gamma)\gg\frac{1}{2}\Gamma X^2|a|^{-2}\mathrm{Re}(a)$. In Figs. 4 and 5, $|a|^{-2}\mathrm{Re}(a)=0.026$ and 0.024, respectively. It is clear from Fig. 5(b) that the asymmetry is reduced as X^2 increases, while for the larger value of $(1-\Gamma)$ in Fig. 5(c) X^2 is never large enough to significantly reduce the asymmetry. Note that this effect must also appear in the spectrum for ordinary resonance fluorescence—obtained by setting $C=0$ in the above results. There $|a|^{-2}\mathrm{Re}(a)=(1+\delta^2)^{-1}$ and the asymmetry should be seen for $X^2\ll 2(1+\delta^2)(1-\Gamma)/\Gamma$.

(3) As in absorptive bistability, far above the instability on the upper branch the incoherent spectrum tends to the Stark triplet of ordinary resonance fluorescence[16] [Figs. 6(a) and 7(a)]. As the instability is approached the sidebands migrate towards the central peak, again following a different course to that in resonance fluorescence.[23] Various behaviors are possible for the same atomic detuning, as evidenced by Figs. 3(b), 4(d), and 5(d). Two features characterize the differences between these examples.

(a) In absorptive bistability the Stark sidebands merge with the central peak before the instability is reached. In dispersive bistability this may or may not be the case. Equation (4.15) gives the linewidths and splitting in the linewidth narrowing region for the spectral components other than the

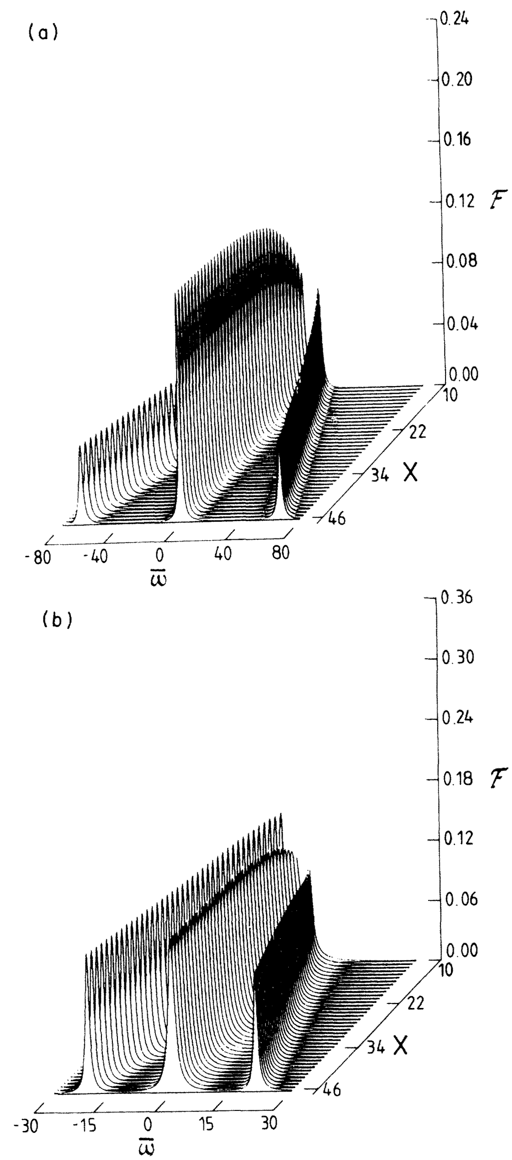

FIG. 6. The incoherent part of the transmitted spectrum along the upper branch showing Rabi sidebands growing relative to the central peak as the instability is approached, $C=20$ and (a) $\delta=1.0$, $\phi=1.0$, $\Gamma=1.00$; (b) $\delta=-1.0$, $\phi=-1.0$, $\Gamma=0.10$.

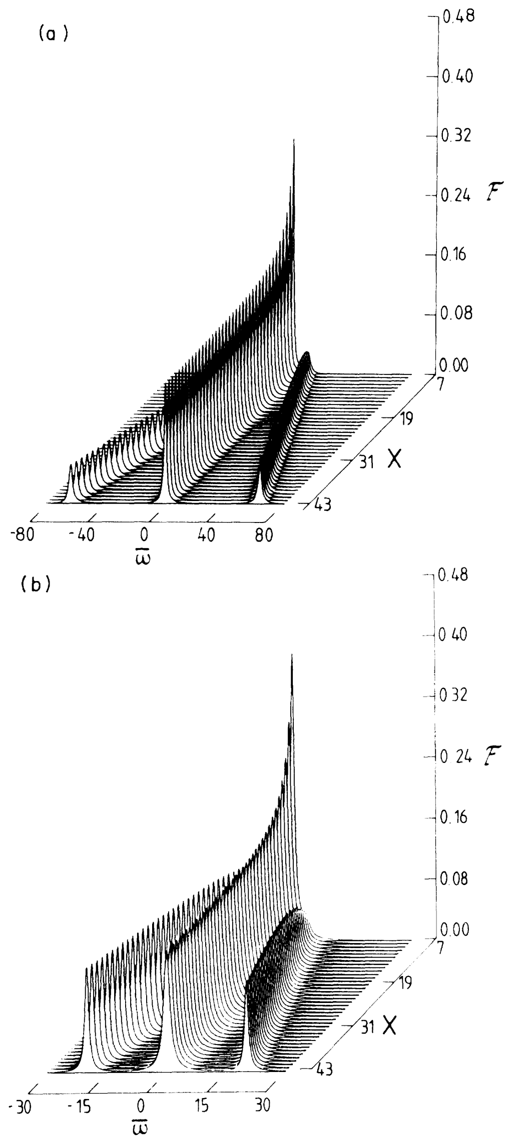

FIG. 7. The incoherent part of the transmitted spectrum along the upper branch showing Rabi sidebands shrinking relative to the central peak as the instability is approached, $C=20$ and (a) $\delta=1.0$, $\phi=-2.0$, $\Gamma=1.00$; (b) $\delta=-1.0$, $\phi=2.0$, $\Gamma=0.10$.

dominant peak. Corresponding to Fig. 4(d), $\lambda_1=4.06$, $\lambda_2=3.06$—the sidebands have merged with the central peak. Corresponding to Figs. 3(b) and 5(d), $\lambda_{1,2}=2.48\pm i\,1.78$ and $\lambda_{1,2}=2.78\pm i\,7.78$, respectively—the sidebands have not merged with the central peak.

(b) In absorptive bistability the sidebands become larger than the central peak immediately before linewidth narrowing sets in [Fig. 2(b)]. Agarwal and Tewari[11] noted that this did not occur when they included dispersion ($\delta\neq 0, \phi=0$). Figures 3(b), 4(d), and 5(d) indicate that, in fact, two different behaviors are possible in dispersive bistability. As the instability is approached along the upper branch, before the region of linewidth narrowing, *either* the sidebands grow at the expense of the central peak *or* the central peak grows at the expense of the sidebands. This distinction is clearly illustrated in Figs. 6(a) and 7(a). The change in relative peak heights is accomplished to varying degrees before linewidth narrowing sets in. In Fig. 3(b) the sidebands have grown, but not quite to the height of the central peak. In Figs. 2(b) and 4(d) they become higher that the central peak.

Note that along the upper branch the incoherent spectrum is not sensitive to small changes in Γ as it is along the lower branch. However, larger changes introduce an asymmetry, as illustrated in Figs. 4(e), 5(e), 6(b), and 7(b).

V. FLUORESCENT SPECTRUM

For absorptive bistability it has recently been shown that the spectrum of the fluorescent light—emitted perpendicular to the direction of propagation—does not exhibit collective features similar to the transmitted spectrum.[14,15] To first order the fluorescent spectrum is just the spectrum of ordinary resonance fluorescence for atoms driven by the mean cavity field. This result may be generalized to dispersive bistability: With the use of the arguments of Ref. 14, and beginning with Eqs. (2.16) (setting $\Gamma_{j_1}=\Gamma_{j_2}=\Gamma_{j_3}=0$) to replace Eqs. (11) and (12) in Ref. 14, only the matrices A and B and steady-state correlations $\gamma^{jj}_{\mu\nu}$ (Ref. 14) are now altered. Again, collective effects will enter only as corrections of order $1/N$ to the spectrum of normal resonance fluorescence, now in a detuned driving field. Including atomic and cavity detunings, the fluorescent spectrum detected at a position $\vec{r}$, summed over atoms at positions $\vec{r}_j$ in an observation volume v—$|\vec{r}-\vec{r}_j|=R_j$, $\vec{r}-\vec{r}_j=R_j\vec{\mathrm{R}}_j$— is given by

$$F_{ss}(\bar{\omega})=F^{ss}_{coh}\delta(\bar{\omega})+F^{ss}_{inc}\mathcal{F}'(\bar{\omega})\ , \tag{5.1}$$

where

$$F^{ss}_{coh}=\sum_{j\in v}\left[\frac{1}{4\pi\epsilon_0}\frac{k_0^2}{R_j}(\vec{\mu}\times\vec{\mathrm{R}}_j)\times\vec{\mathrm{R}}_j\right]^2\tfrac{1}{2}\Gamma(1+\delta^2)X^2/(1+\delta^2+X^2)^2\ , \tag{5.2}$$

$$F_{\rm inc}^{\rm ss}=\sum_{j\in v}\left[\frac{1}{4\pi\epsilon_0}\frac{k_0^2}{R_j}(\vec{\mu}\times\vec{\rm R}_j)\times\vec{\rm R}_j\right]^2\frac{1}{2}\left[1-\Gamma\frac{1+\delta^2}{1+\delta^2+X^2}\right]X^2/(1+\delta^2+X^2)\ , \tag{5.3}$$

and

$$\mathscr{F}'(\bar{\omega})=\frac{1}{2\pi}f'^{-1}\,|\,\Lambda'(i\bar{\omega})\,|^{-2}2\,{\rm Re}(\Lambda'(i\bar{\omega})\{c'(b'^*e'-b'f')+(a'+i\bar{\omega})[(d'+i\bar{\omega})f'-b'^*g']\})\ , \tag{5.4}$$

$$\Lambda'(i\bar{\omega})=(a'-i\bar{\omega})(a'^*-i\bar{\omega})(d'-i\bar{\omega})-b'c'(a'^*-i\bar{\omega})-b'^*c'^*(a'-i\bar{\omega})\ , \tag{5.5}$$

with

$$\begin{aligned} a'&=1+i\delta\ ,\\ b'&=i\sqrt{2\Gamma}Xe^{i\phi_x}\ ,\\ c'&=i\sqrt{\Gamma/2}Xe^{-i\phi_x}\ ,\\ d'&=2\Gamma\ , \end{aligned} \tag{5.6}$$

and

$$e'=\tfrac{1}{2}\Gamma\frac{1-i\delta}{1+i\delta}$$

$$\times e^{2i\phi_x}X^2(1+\delta^2)/(1+\delta^2+X^2)^2\ ,$$

$$f'=\tfrac{1}{2}\left[1-\Gamma\frac{1+\delta^2}{1+\delta^2+X^2}\right]X^2/(1+\delta^2+X^2)\ , \tag{5.7}$$

$$g'=-i\tfrac{1}{2}\sqrt{\Gamma/2}(1-i\delta)e^{i\phi_x}X^3/(1+\delta^2+X^2)^2\ .$$

Note that the only dependence on the cavity detuning ϕ is in the determination of the mean cavity field intensity X^2 via Eq. (2.27).

VI. PHOTON ANTIBUNCHING

One of the most interesting results coming from the study of ordinary resonance fluorescence has been the prediction[24] and observation[25] of photon antibunching in the fluorescence from a single atom. Casagrande and Lugiato have looked for photon antibunching in absorptive bistability.[9] Using the quantum-statistical theory developed by Gronchi and Lugiato,[7,12] for purely radiative atomic decay ($\Gamma=1$) they find antibunching along the lower branch, in both the "good cavity" and "bad cavity" limits. For the "bad cavity" limit we may now extend this investigation to dispersive bistability.

The normalized second-order correlation function for the transmitted light is given by

$$\begin{aligned} g_{\rm ss}^{(2)}(0)&=\langle a^{\dagger 2}a^2\rangle_{\rm ss}/\langle a^\dagger a\rangle_{\rm ss}^2\\ &={\rm av}(\alpha_2^2\alpha_1^2)_{\rm ss}/{\rm av}(\alpha_2\alpha_1)_{\rm ss}^2\ , \end{aligned} \tag{6.1}$$

and after adiabatic elimination of the field variables [Eqs. (2.15)], and linearization about the steady state [Eq. (2.18)]

$$g_{\rm ss}^{(2)}(0)-1=(1/N\Gamma)8C^2(1+\phi^2)^{-1}\left[2N\langle\tilde{J}_+\tilde{J}_-\rangle_{\rm ss}/X^2-{\rm Re}\left[\frac{1-i\phi}{1+i\phi}e^{-2i\phi_x}2N\langle\tilde{J}_-\tilde{J}_-\rangle_{\rm ss}/X^2\right]\right]\ . \tag{6.2}$$

In the derivation of Eq. (6.2) odd moments—e.g., ${\rm av}(\tilde{j}_2\tilde{j}_1^2)_{\rm ss}$—vanish since the $\tilde{j}_\mu$ are Gaussian distributed, and the term ${\rm av}(\tilde{j}_2^2\tilde{j}_1^2)_{\rm ss}=\langle\tilde{J}_+^2\tilde{J}_-^2\rangle_{\rm ss}$ has been dropped as it is of order $1/N^2$.

Using Eq. (6.2) and the results for $\langle\tilde{J}_+\tilde{J}_-\rangle_{\rm ss}$ and $\langle\tilde{J}_-\tilde{J}_-\rangle_{\rm ss}$ calculated in Sec. III, we may evaluate $g_{\rm ss}^{(2)}(0)-1$ for arbitrary atomic and cavity detunings. For absorptive bistability ($\delta=\phi=0$) we recover the result published by Casagrande and Lugiato.[9] A typical example of results showing photon antibunching—$g_{\rm ss}^{(2)}(0)-1<0$—for nonzero atomic and cavity detunings is given in Fig. 8. As Casagrande and Lugiato observed, photon antibunching occurs along the lower branch for $\Gamma=1$, and is reduced and eventually eliminated as Γ decreases. In the limit $\Gamma\to 0$,

$$N\Gamma[g_{\rm ss}^{(2)}(0)-1]=8C^2/[(1+\phi^2)X^2+(1+\delta^2)(1+\phi^2+2C)]\ , \tag{6.3}$$

which is just twice the expression for $N\Gamma T_{\rm inc}^{\rm ss}/T_{\rm coh}^{\rm ss}$ in this limit [Eq. (3.20)]. We have not plotted $g_{\rm ss}^{(2)}(0)-1$ along the upper branch, as there photon antibunching does not occur and the behavior is similar to that in Fig. 1(b).

Antibunching appears to be strongest at $X^2=0$ and it is useful to view the general result for $g_{ss}^{(2)}(0)-1$ in the weak-field limit $X^2 \ll 1+\delta^2$,

$$g_{ss}^{(2)}(0)-1=(1/N\Gamma)8C^2(1+\delta^2)^{-1}(1+\phi^2)^{-1}\left[(1-\Gamma)\left[1+\frac{2C}{1+\phi^2}\right]^{-1}-\Gamma(1+\phi^2)^{-1}\right.$$
$$\left.\times\frac{(1-\delta^2)(1-\phi^2)-4\delta\phi+2C(1-\delta\phi)}{[1+2C/(1+\phi^2)]^2+[\delta-\phi 2C/(1+\phi^2)]^2}\right]. \tag{6.4}$$

For $\delta=-\phi$ (including absorptive bistability, $\delta=\phi=0$) this reduces to

$$g_{ss}^{(2)}(0)-1=(1/N\Gamma)8C^2(1-2\Gamma)\left[1+\frac{2C}{1+\phi^2}\right]^{-1} \tag{6.5}$$

and photon antibunching occurs for $0.5<\Gamma\le 1$. More generally, the appearance, or not, of photon antibunching is determined by competition between the terms in Eq. (6.4) with coefficients $(1-\Gamma)$ and Γ. The former is always positive, and hence, for any C, δ, and ϕ the largest effect occurs for $\Gamma=1$, as observed in Fig. 8. However, photon antibunching may not occur, even for $\Gamma=1$, depending on the sign of the term with coefficient Γ. For each C and Γ, setting $g_{ss}^{(2)}(0)-1=0$ gives a quadratic in δ whose roots $\delta_{1,2}^{C,\Gamma}(\phi)$ define a boundary in (δ,ϕ) space separating regions of photon antibunching and no photon antibunching—for $\Gamma=1$,

$$\delta_{1,2}^{C,\Gamma}(\phi)=(1-\phi^2)^{-1}\{-(C+2)\phi\pm[(1+\phi^2)(1+\phi^2+2C)+\phi^2C^2]^{1/2}\}. \tag{6.6}$$

Figure 9(a) illustrates this subdivision of (δ,ϕ) space for $\Gamma=1$ and $C=20$. As Γ decreases the area in (δ,ϕ) space for photon antibunching eventually shrinks to zero. For each C, antibunching occurs for some (δ,ϕ) if

$$\Gamma>4(C+2)/(C+4)^2. \tag{6.7}$$

If $\Gamma\le 4(C+2)/(C+4)^2$ no photon antibunching occurs, for any (δ,ϕ). Note, for $C>0$,

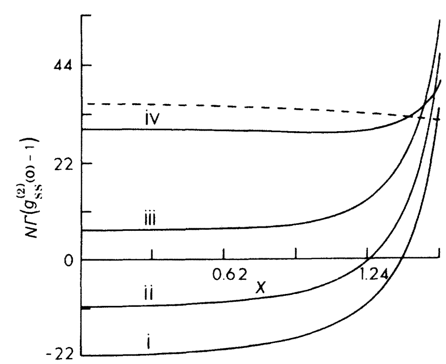

FIG. 8. Photon antibunching along the lower branch for $C=20$, $\delta=1.0$, $\phi=-2.0$, and (i) $\Gamma=1.00$, (ii) $\Gamma=0.80$, (iii) $\Gamma=0.50$, and (iv) $\Gamma=0.10$. The dashed curve is for the limit $\Gamma\to 0$ [Eq. (6.3)].

$4(C+2)/(C+4)^2<0.5$ and photon antibunching therefore persists in dispersive bistability after it has been eliminated in absorptive bistability. This is illustrated by the subdivision of (δ,ϕ) space in Fig. 9(b).

VII. SUMMARY AND CONCLUSIONS

We have used the quantum-statistical theory of optical bistability developed in OBII (Ref. 1) to calculate steady-state correlations, and the spectrum and second-order correlation function for the transmitted light in both absorptive and dispersive bistability in a low-Q cavity.

These calculations are based on a Fokker-Planck equation derived in the positive P representation.[5] This representation gives explicitly positive-semidefinite diffusion; an important property, since for optical bistability, the Fokker-Planck equation derived following Haken's laser theory[4] has nonpositive-definite diffusion.[12,13] The outcome of our formalism is, however, that expressions for steady-state correlations and spectra which naively overlook this nonpositive-definite diffusion are, in fact, correct. Using these expressions, for absorp-

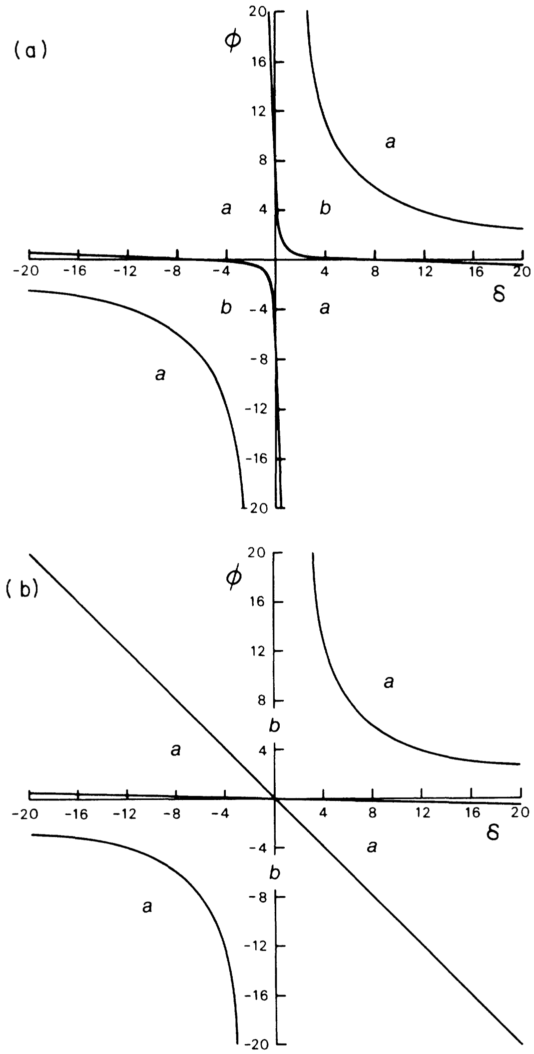

FIG. 9. The subdivision of (δ,ϕ) space into regions of photon antibunching and no photon antibunching in the weak-field limit for $C=20$. The solid curves mark boundaries where $g_{ss}^{(2)}(0)-1=0$. Regions labeled a have $g_{ss}^{(2)}(0)-1<0$ and regions labeled b have $g_{ss}^{(2)}(0)-1>0$: (a) $\Gamma=1.00$, (b) $\Gamma=0.5$.

tive bistability our results agree with those of Agarwal *et al.*,[6] Lugiato,[7] and Casagrande and Lugiato,[9] who use quite different methods.

For dispersive bistability the transmitted spectrum exhibits collective features similar to those in absorptive bistability; however, there are a number of differences in detail. The broad collective component along the lower branch is generally a doublet, with its collective linewidth modified by the cavity detuning. This doublet is very sensitive to phase destroying atomic collisions. For weak incident intensities, small departures from purely radiative decay introduce a dramatic asymmetry. Along the upper branch, for the same atomic detuning and different cavity detunings, the Rabi sidebands may either grow or shrink with respect to the central peak as the bistability region is entered from above—they may or may not merge with the central peak before the upper instability is reached.

Photon antibunching occurs along the lower branch in dispersive bistability for a wide range of atomic and cavity detunings. The largest effect is for purely radiative damping, and with the inclusion of collisions there exists a value of the collisional decay rate beyond which antibunching does not occur. Generally photon antibunching remains in dispersive bistability—for some atomic and cavity detunings—when the effect in absorptive bistability has already been destroyed.

ACKNOWLEDGMENTS

One of us (H.J.C.) thanks the Center for Studies in Statistical Mechanics, University of Texas at Austin, where much of the numerical work was done, for support on a grant from the Robert A. Welch foundation. The research reported here has been supported in part by the United States Army through its European Research Office.

[1]P. D. Drummond and D. F. Walls, Phys. Rev. A 23, 2563 (1981).
[2]R. Bonifacio and L. A. Lugiato, Lett. Nuovo Cimento 21, 505 (1978).
[3]H. J. Carmichael and J. A. Hermann, Z. Phys. B 38, 365 (1980).
[4]H. Haken, *Encyclopedia of Physics* (Springer, Berlin, 1970), Vol. XXV/2C, pp. 60–71, 153–156.
[5]P. D. Drummond and C. W. Gardiner, J. Phys. A 13, 2353 (1980); P. D. Drummond, C. W. Gardiner, and D. F. Walls, Phys. Rev. A 24, 914 (1981).
[6]G. S. Agarwal, L. M. Narducci, R. Gilmore, and Da Hsuan Feng, Phys. Rev. A 18, 620 (1978).
[7]L. A. Lugiato, Nuovo Cimento B50, 89 (1979).
[8]L. M. Narducci, R. Gilmore, Da Hsuan Feng, and G. S. Agarwal, Opt. Lett. 2, 88 (1978).
[9]F. Casagrande and L. A. Lugiato, Nuovo Cimento B55, 173 (1980).
[10]For two reviews see D. F. Walls, Nature 280, 451 (1979); R. Loudon, Rep. Prog. Phys. 43, 913 (1980).
[11]G. S. Agarwal and S. P. Tewari, Phys. Rev. A 21, 1638 (1980).
[12]M. Gronchi and L. A. Lugiato, Lett. Nuovo Cimento 23, 593 (1978).

[13]G. S. Agarwal, L. M. Narducci, Da Hsuan Feng, and R. Gilmore, Phys. Rev. A 21, 1029 (1980).

[14]H. J. Carmichael, Z. Phys. B 42, 183 (1981).

[15]L. A. Lugiato, Lett. Nuovo Cimento 29, 375 (1980).

[16]B. R. Mollow, Phys. Rev. 188, 1969 (1969); H. J. Carmichael and D. F. Walls, J. Phys. B 9, 1199 (1976); H. J. Kimble and L. Mandel, Phys. Rev. A 13, 2123 (1976); C. Cohen-Tannoudji and S. Reynaud, J. Phys. B 10, 345 (1977).

[17]F. Schuda, C. R. Stroud, Jr., and M. Hercher, J. Phys. B 7, L198 (1974); F. Y. Wu, R. E. Grove, and S. Ezekiel, Phys. Rev. Lett. 35, 1426 (1975); W. Hartig, W. Rasmussen, R. Schieder, and H. Walther, Z. Phys. A 278, 205 (1976).

[18]Note that the operator $\hat{D}$ (complex variable D) in OB II (Ref. 1) corresponds to $2J_z(2j_3)$. Also we have omitted a term describing thermal fluctuations in the cavity field from Eq. (2.5).

[19]The "bad-cavity" limit requires $\kappa \gg \gamma_{\|}, \gamma_{\perp}$. The cavity Q is low only in this sense; a broad cavity resonance relative to atomic linewidths. Strictly, this condition should be met without lowering the cavity finesse. The requirement $R \simeq 1$ is introduced by the mean-field limit (Refs. 2 and 3) and is implicitly assumed by all quantum statistical theories (Refs. 1, 6–9, and 11–15) where the cavity field is described by a single mode with weak coupling to its environment (at the mirrors).

[20]S. S. Hassan, P. D. Drummond, and D. F. Walls, Opt. Commun. 27, 480 (1978); G. P. Agrawal and H. J. Carmichael, Phys. Rev. A 19, 2074 (1979); R. Bonifacio, M. Gronchi, and L. A. Lugiato, Nuovo Cimento B53, 311 (1979).

[21]M. Lax, Rev. Mod. Phys. 32, 25 (1960); C. W. Gardiner, *A Handbook of Stochastic Methods* (Springer, Berlin, 1982).

[22]Following the method used in OB II (Ref. 1), the relationship between the six-dimensional Fokker-Planck equation [Eq. (3.2)] and Eq. (2.19)—and consequently between Eqs. (3.6) and (3.8) and Eqs. (4.3) and (4.5)—may be established via corresponding stochastic differential equations. Stochastic differential equations in the six-dimensional ($\vec{\vec{j}}_x, \vec{\vec{j}}_y$) space are equivalent to a set of equations with complex noise in the three-dimensional complex $\vec{\vec{j}}$ space. These have drift and diffusion matrices which follow via the usual relationships from Eq. (2.19) if a complex square root $B = B^x + iB^y$ [Eq. (3.4)] is admitted to accommodate the nonpositive-definiteness of $D = BB^T$.

[23]The incoherent spectrum for resonance fluorescence with a detuned driving field may be plotted from the results in Sec. V. In principle, it is expandable as in Eq. (4.10) where the λ_μ are now roots of the cubic $\Lambda'(\lambda)=0$. For $X^2 \ll 1+\delta^2$, and all Γ and $\delta \neq 0$, one root λ_3 is real and $\lambda_{1,2}$ are complex conjugates. The spectrum is given by Eqs. (4.10)–(4.12) with $C=0$—a doublet, which may or may not be resolved depending on δ. Then the behavior as X^2 increases follows one of two possible courses depending on δ and Γ. For each Γ there is a critical detuning $|\delta|_c$ (for $\Gamma = \frac{1}{2}$, $|\delta|_c = 0$). (1) *For* $|\delta| < |\delta|_c$ intensities $X_1{}^2$ and X_2^2 exist at which the λ_μ are all real and $\lambda_2 = \lambda_3$; as X^2 increases from zero first the doublet coalesces into a single peak at $X^2 = X_1^2$; a single peak remains for $X_1^2 < X^2 < X_2^2$; for $X^2 > X_2^2$ the familiar Stark-split spectrum develops in much the same way as in the resonant case (Ref. 16), (2) for $|\delta| > |\delta|_c$ a pair of complex-conjugate roots $\lambda_{1,2}$ exists for all values of X^2; the Stark triplet develops with the growth of a central peak between the peaks of the doublet. (See Kimble and Mandel, Ref. 16.)

[24]H. J. Carmichael and D. F. Walls, J. Phys. B 9, L43 (1976).

[25]H. J. Kimble, M. Dagenais, and L. Mandel, Phys. Rev. Lett. 39, 691 (1977).